Hindawi
Geofluids
Volume 2020, Article ID 8893299, 12 pages
https://doi.org/10.1155/2020/8893299

Research Article

Experimental Investigation into the Influences of Weathering on the Mechanical Properties of Sedimentary Rocks

Xiaoshuang Li,[1,2,3,4] Yingchun Li ,[5] and Saisai Wu [1]

[1]School of Resources Engineering, Xian University of Architecture and Technology, Xian 710000, China
[2]China Steel Group Ma On Shan Mine Research Institute Co. LTD., Maanshan 243000, China
[3]State Key Laboratory of Safety and Health in Metal Mines, Maanshan, Anhui 400045, China
[4]Jiangxi Key Laboratory of Mining Engineering, Jiangxi University of Science and Technology, Ganzhou 341000, China
[5]State Key Laboratory of Coastal and Offshore Engineering, Dalian University of Technology, Dalian 116024, China

Correspondence should be addressed to Saisai Wu; saisai.wu@xauat.edu.cn

Received 2 June 2020; Revised 13 October 2020; Accepted 17 November 2020; Published 8 December 2020

Academic Editor: Fabien Magri

The time-dependent behaviors of the sedimentary rocks which refer to the altering of the mechanical and deformable properties of rock elements in the long-term period are of increasing importance in the investigation of the failure mechanism of the rock strata in underground coal mines. In order to obtain the accurate and reliable mechanical parameters of the sedimentary rocks at different weathering grades, the extensive experimental programs including the Brazilian splitting test, uniaxial compression tests, and direct shear tests have been carried out on the specimens that exposed to the nature environments at different durations. The correlation between the weathering grades and mechanical parameters including uniaxial tensile strength, uniaxial compression strength, elastic modulus, Poisson's ratio, cohesion, and friction coefficient was proposed. The obtained results suggested that uniaxial tensile strength, uniaxial compressive strength, elastic modulus, and cohesion dramatically decreased with increasing weathering time, characterized as the negative exponential relationship in general. The influences of various weathering grades on fracture behavior of the rock specimens were discussed. The cumulative damage of the rock by the weathering time decreased the friction coefficient of the specimens which led to the initiation and propagation of microcrack within the rock at lower stress conditions. The obtained results improved the understanding of the roles of weathering on the mechanical properties of sedimentary rocks, which is helpful in the design of the underground geotechnical structures.

1. Introduction

In the underground mining projects, the time-dependent mechanical properties of rock mass are the basic engineering parameters to investigate the rock strata movement as well as the stability of rock mass [1–3]. Due to the differences in compositions, structures, and the ages of formation, the time-dependent mechanical properties or fracture conditions of different rocks are different [4–6]. The mechanical properties of rocks are also affected by other factors including weathering time, temperature, humidity, and the surrounding medium [7, 8]. The difference in the time-dependent mechanical properties of the rock would result in the different failure mechanisms of the rock strata in underground mines [9–11]. For underground coal mines, the rock types that surrounding the coal seam are generally characterized as the sedimentary rocks, which have the characteristics of low strength, good integrity, and fast weathering [12].

Weathering is a typically time-dependent process and regarded as the procedure of degradation of rocks by physical and chemical effects. The ongoing process of weathering in nature produces progressive but intricate alterations in the petrographical, mineralogical, microstructural, and geomechanical characteristics of rocks [13]. Generally, the weathering process decreases the rock strength by increasing the deformability and degradation of the rock [14]. Since the negative influences of the weathering on the strength and deformational properties of rocks, a critical evaluation of the physical-mechanical behavior of rocks under the effects of weathering are of significant relevance in underground mines [15, 16]. Previous studies in the assessment of the geotechnical condition of a railway tunnel found that the weathering could cause significant issues and resulted in huge economic losses [17].

A number of studies have been carried to assess the influences of weathering process on the mechanicals of granitoid rocks [18–20]. Heidari et al. [21] reported that the elastic modulus of granodiorite decreased with increasing the weathering time. Based on the correlation between the weathering grades and change in mechanical and petrographic properties, Momeni et al. [22] attempted to propose the weathering classification for granitoid rocks. Alavi Nezhad Khalil Abad et al. [23] studied the characteristics of granitic rock mass in various weathering zones in tropical environments. Other researchers found that the weathering process decreased the elastic modulus of rock by altering the mineralogical characteristics of the rock. For the calcareous rocks, the elastic modulus has a negative exponential relationship with the calcite content [24].

Momeni et al. [25] reported that the difference in the compressive strength and elastic modulus for the fresh and weathered rock is related to their petrographical properties. The appearances of clay minerals with crack density were recognized as the most effective parameters instead of primary mineral composition and textural properties [12]. However, the aforementioned researches mostly focused on studying the effects of weathering on granitoid rocks. Discussions on the time-dependent behavior of sedimentary rocks affected by weathering are found to be reported rarely in the literature. For the underground coal mines, the rock types that surrounding the coal seam are generally characterized as the sedimentary rocks. As one of the typical types of sedimentary rocks, black shale is formed by dehydration and cementation of clay. It is predicted that the mechanical parameters of black shale will be significantly affected by weathering processes. Therefore, it is necessary to study the evolution law of physical and mechanical parameters of black shale in the process of weathering.

In this study, the time-dependent behaviors of sedimentary rocks were examined and assessed at a certain duration of weathering through extensive experimental programs. The correlation between the weathering grades and mechanical parameters including uniaxial tensile strength, uniaxial compression strength, elastic modulus, Poisson's ratio, cohesion, and friction coefficient was proposed. The influences of various weathering grades on the behavior of the rock specimens were discussed, whereby a more reasonable design of the geotechnical engineering structures considering the effects of weathering, especially for the design of slope angle and boundary, could be conducted.

2. Experimental Programs

2.1. Specimens. The tested black shale specimens which are a typical type of sedimentary rocks were collected from an underground mine. The black shale is formed by dehydration and cementation of clay and has the characteristics of fine grain, dense, low strength, good integrity with little small cracks, and fast weathering. The specimens are prepared through drilling vertically in the direction of the rock layer with good integrity. The diameter of the drilled cylinder core is 50 mm. For the uniaxial compression test, the ratio of height to diameter of the specimens is 2. For the direct shear mechanical test, the ratio of height to diameter is 1. The ratio of height to diameter is 0.5 for the Brazilian split test. The surfaces of the specimens were polished by a grinder. The parallelism deviation of the surfaces at both ends of the specimen was controlled less than 0.1 millimeters. The diameter deviation along the surface of the specimens was less than 0.1 millimeters, which was checked with a cursor caliper. The specimens used for each test are shown in Figure 1.

2.2. Testing Devices. In order to evaluate the influences of the weathering on the uniaxial tensile strength of rock, the Brazilian split tests were carried out on the specimens that were exposed to the environments at different duration. The dimension of the cylinder specimens for the Brazilian split tests is 50 mm × 25 mm. The Brazilian split tests are one of the common methods to determine the uniaxial tensile strength of rock. As shown in Figure 2, the electro-hydraulic servo pressure tester was used to perform the Brazilian split tests. During the tests, a relative linear increasing load at 0.50 kN per second in the direction of the diameter was applied, until the failure occurred. A schematic diagram of the loading method is shown in Figure 2(b). The uniaxial tensile strength of the specimens is the ratio applied longitudinal force at the failure time and the cross-sectional area perpendicular to the loading direction.

The uniaxial compression tests were conducted on the cylinder specimens that were exposed to environments with different duration to determine the effects of weathering time on the uniaxial compression strength of rock. The dimension of specimens used for uniaxial compression tests is 50 mm × 100 mm. During the tests, the compression stresses applied on the specimens were increased approximately linearly at 1.0 kN per second until the occurrence of the failure. When compression failure occurred under the action of uniaxial force, the uniaxial compressive strength of rock is the ratio of the maximum load at failure to the cross-sectional area perpendicular to the loading direction. The arrangement of the uniaxial compression testing system is shown in Figure 3.

The influences of the weathering time on the shear strength, internal friction angle, and cohesion of the specimens were determined through conducting the direct shear tests on the specimens with different exposure time to the environments. The dimensions of the cylinder specimens used for the direct shear tests were 50 mm × 50 mm. During the direct shear tests, a relative linear increasing shear load at 0.50 kN per second along the direction of the diameter of the specimens was applied while under different compressive stress, until the failure occurred. The arrangement of the direct shear testing system is shown in Figure 4.

2.3. Testing Procedures. After the specimens were prepared, all specimens were tagged and photographed. The specimens were then carefully placed in the open environment so that the specimens were weathered in the natural state. To accurately determine the effects of weathering on the mechanical

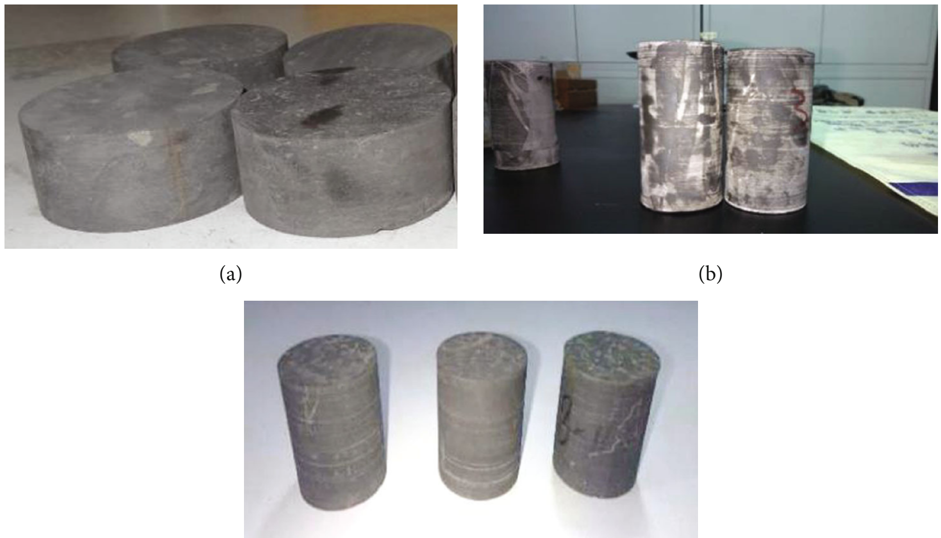

(a) (b) (c)

Figure 1: Examples of the specimen: (a) Brazilian split test; (b) uniaxial compression test; and (c) direct shear tests.

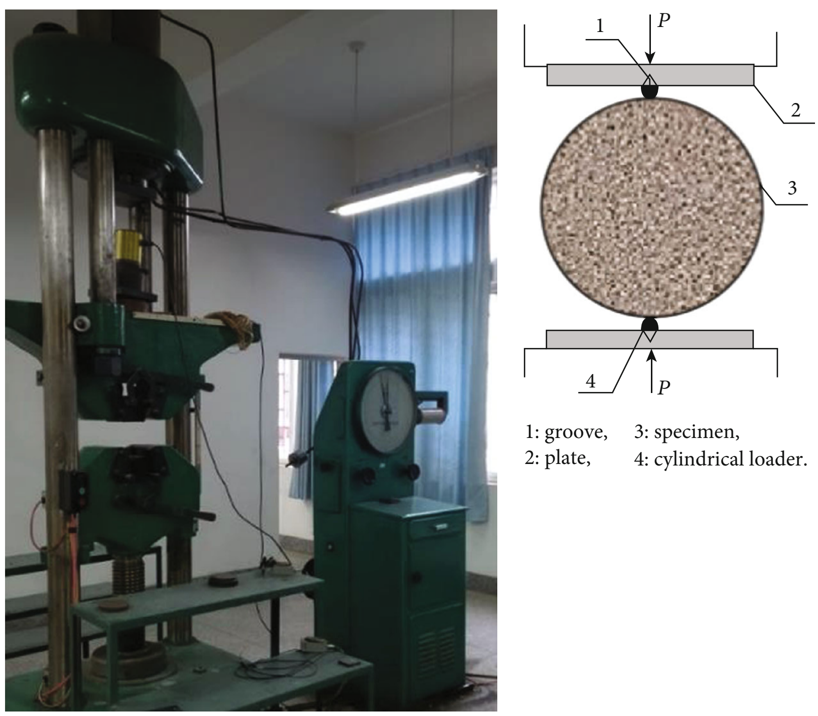

(a) (b)

Figure 2: Brazilian split test equipment: (a) electro-hydraulic servo pressure tester and (b) schematic diagram of the loading method.

properties of the specimens, the ageing of the rock specimens was examined and evaluated at intervals of one week. The longest duration of the weathering was four weeks. Considering that the black shale has the characteristics of low strength, good integrity, and fast weathering, 28 days' exposure to the environments was considered to be a sufficient period for the occurrence of measurable change on the mechanical properties of the specimens. After each interval, Brazilian split tests, uniaxial compression tests, and direct shear tests were carried out to determine the relevant physical and mechanical parameters of the specimens. During the tests, the stresses applied on the specimens were increased approximately linearly until the occurrence of the failure. The arrangements of the experimental programs are shown in Table 1. It should be noted that to eliminate the effects of any scatter on the test results, three specimens were tested in each condition. The specimens without the exposure duration to the environments were conducted as the reference tests.

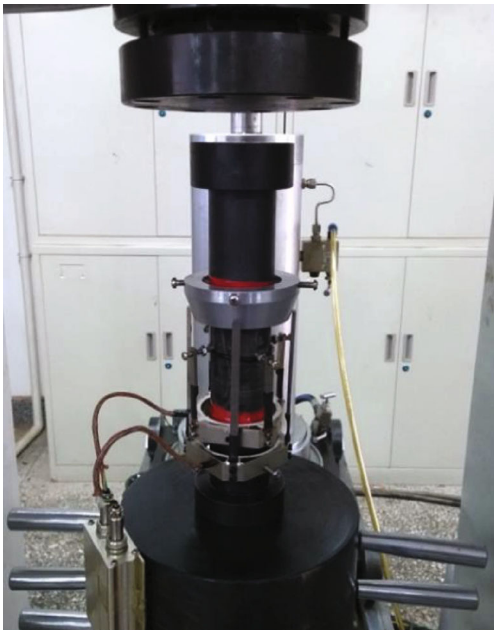

Figure 3: Uniaxial compression testing system.

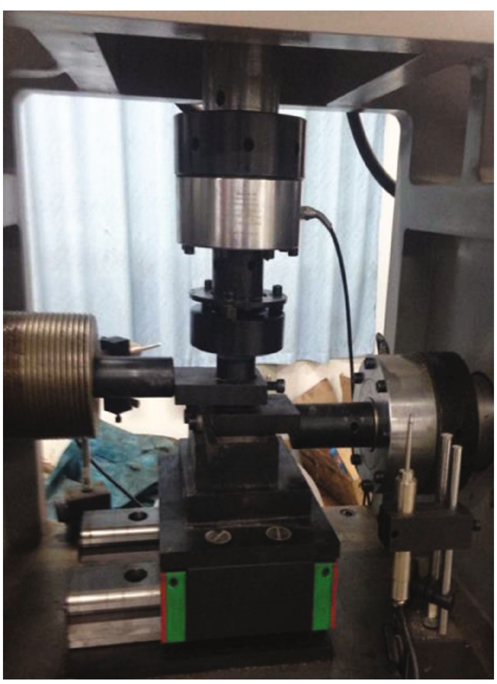

Figure 4: The direct shear testing system.

3. Testing Results

3.1. Brazilian Split Tests. During the tests, the stresses applied on the specimens were increased approximately linearly. One of the failed specimens is shown in Figure 5. The failure mode of the specimens in the Brazilian split tests was characterized by a dominant tensile fracture along the vertical direction with little small cracks. The ultimate tensile strength of the specimens could be calculated from the failure load using the following equation (1). The variation in the average ultimate tensile strength of the specimens with weathering time is presented in Table 2. The results showed that the ultimate tensile strength of the specimens decreased with the increasing of weathering time. At the weathering time of 28 days, the calculated ultimate tensile strength of the specimens was around 2.98 MPa. While for the specimens without exposure to the environments, the calculated strength was 9.82 MPa which was more than three times of the specimens at the weathering time of 28 days. This indicated that the weathering process could significantly decrease the strength of the specimen within the duration of one month.

Table 1: The design of the experimental programs.

ID	Weathering period (days)	Number of specimens		
		Brazilian split test	Uniaxial compression tests	Direct shear tests
1	0	3	3	3
2	7	3	3	3
3	14	3	3	3
4	21	3	3	3
5	28	3	3	3

$$\sigma_t = \frac{2P}{\pi d t}, \qquad (1)$$

where σ_t is the ultimate tensile strength, MPa; P is the ultimate pressure of specimen at failure, N; and d and t are the diameter and thickness of the specimen, mm.

3.2. Uniaxial Compressive Stress. During the tests, the compression stresses applied on the specimens were increased approximately linearly until the occurrence of the failure. One of the failed specimens in the uniaxial compression tests is shown in Figure 6. When the specimen was finally destroyed, an obvious crack was produced along the axial direction with several small horizontal cracks along the horizontal direction. Based on the test results, elastic modulus and Poisson's ratio were calculated. The relationship between the ultimate compression strength, elastic modulus, and Poisson's ratio with weathering time are presented in Table 3. Although the uniaxial compression strength of the specimens varied with the weathering time, the test results at a particular weathering time remained reasonably consistent and repeatable.

It can be seen from the test results that the weathering time has significant influences on the mechanical properties of the specimens under the uniaxial compression test. At the weathering time of 28 days, the average ultimate compression strength, elastic modulus, and Poisson's ratio of the specimens are 12.36 MPa, 3.55 GPa, and 0.39, respectively. While for the specimens without the exposure duration to the environments, the strength, elastic modulus, and Poisson's ratio of the specimens are 66.48 MPa, 13.29 GPa, and 0.16. The significant difference in the mechanical properties of the specimens at the condition of 4 weeks' weathering time and without the weathering also demonstrated the

Figure 5: The failed specimen in the Brazilian split tests.

Figure 6: The failed specimen in the uniaxial compression tests.

Table 2: The variation in the ultimate tensile strength with weathering time.

Weathering time (days)	Test case	Uniaxial tensile strength (MPa)	Mean value (MPa)	Standard deviation (MPa)	Relative standard deviation (%)
	Case 1-1	9.75			
0	Case 1-2	9.12	9.82	0.51	5.23
	Case 1-3	10.59			
	Case 2-1	6.53			
7	Case 2-2	6.72	6.91	0.38	5.50
	Case 2-3	7.48			
	Case 3-1	4.72			
14	Case 3-2	4.81	5.09	0.45	8.84
	Case 3-3	5.74			
	Case 4-1	3.75			
21	Case 4-2	3.98	4.02	0.21	5.15
	Case 4-3	4.33			
	Case 5-1	2.68			
28	Case 5-2	2.97	2.98	0.21	6.94
	Case 5-3	3.29			

direct effects of weathering on the mechanical properties of specimens.

3.3. Direct Shear Tests. For the direct shear tests, the shear stress applied on the specimens was increased approximately linearly while under different compressive stress. Some of the failed specimens in the direct tests are shown in Figure 7. As shown in Figure 7, when the specimen failed, an obvious shear crack was produced in the horizontal direction. The angle between the path of crack growth and the transverse plane was usually around 30 degrees. According to Mohr Coulomb's law, the relationship between the shear stress and the compressive stress can be characterized as equation (2). From the equation, it can be seen that under a particular weathering time, the correlation between the compressive forces and corresponded shear strength at the same time can be drawn by a straight line. The intercept of the fitted straight line on the ordinate is cohesion, and the inclination of the straight line is the internal friction angle. Using this method, the cohesion and internal friction angle of the specimens under a particular weathering time were calculated.

$$\tau = C + \sigma \tan \Phi, \tag{2}$$

where: τ is the shear strength of specimen, MPa;

C is cohesion, MPa;

σ is the compressive stress applied on the specimen, MPa;

Φ is the angle of internal friction, degree.

The variations in the mechanical parameters with weathering time in the direct shear tests are displayed in Table 4. It should be noted that three specimens were tested in each condition and the test results at a particular testing condition remained reasonably repeatable. Only the average values of the shear strength, the internal friction angle, and cohesions are displayed in Table 4. From the test results, it can be seen that under certain compressive stress, the weathering time has significant effects on the shear strength of the specimens. Under the compressive stress of 10 MPa, the average shear strength of the specimens with weathering a time of 7 and 28 days are 8.48 and 4.49 MPa, respectively. Under the compressive stress of 25 MPa, the shear strength of the specimens with weathering time of 7 and 28 days are 16.14 and 10.73 MPa, respectively.

Table 3: The variation of mechanical parameters with weathering time under the uniaxial compression conditions.

Weathering time (days)	Test case	Uniaxial compression strength (MPa)	Mean value (MPa)	Standard deviation (MPa)	Relative standard deviation (%)	Elastic modulus (GPa)	Poisson's ratio
0	Case 1-1	61.15	66.48	4.21	6.33	13.29	0.160
	Case 1-2	65.49					
	Case 1-3	72.80					
7	Case 2-1	36.42	39.51	2.06	5.21	4.70	0.295
	Case 2-2	39.79					
	Case 2-3	42.32					
14	Case 3-1	20.98	24.25	2.18	8.99	4.34	0.339
	Case 3-2	24.89					
	Case 3-3	26.88					
21	Case 4-1	13.52	15.29	1.18	7.72	3.92	0.379
	Case 4-2	17.03					
	Case 4-3	4.33					
28	Case 5-1	8.87	10.09	0.81	8.03	3.55	0.408
	Case 5-2	10.13					
	Case 5-3	11.27					

Figure 7: Examples of the failed specimen in the direct share tests.

4. Analysis and Discussion

4.1. Results Analysis. Because of the long time, high cost, and many other influencing factors including the influence of joint fissure, rock mass structure, groundwater, and size effect in rock mass, it is difficult to obtain the macromechanical parameters of the rock mass. Therefore, to provide the basic rock mechanical properties for the design of the engineering project, the mechanical parameters of rock mass are reduced and modified to the mechanical parameters of rock specimen. In this study, based on the comprehensive experimental tests, the uniaxial tensile strength, uniaxial compressive strength, elastic modulus, Poisson's ratio, cohesion, and angle of internal friction of black shale at different weathering time were obtained through Brazilian split tests, uniaxial compression tests, and direct shear tests. The results of the above tests are summarized in Table 5.

The average uniaxial tensile and uniaxial compressive strength values of the specimen at different weathering times are plotted in Figure 8. From Figure 8, it is clear that with the increasing of the weathering time, both the uniaxial tensile strength and uniaxial compressive strength values of the specimen gradually decreased. Compared to the specimens without exposure to the environments, the uniaxial tensile and uniaxial compressive strength values at weathering time of 28 days decreased by 2.30 times and 5.59 times, respectively. The trendlines are plotted in Figure 8 to represent the variations of the strength values with the weathering time. The determination coefficient (R^2) of the plotted trendlines are provided in Figure 8. Generally, the uniaxial tensile and uniaxial compressive strength values showed negative exponential behavior at the weathering time ranging from 0 to 28 days.

Table 4: The variation of mechanical parameters with weathering time in direct shear tests.

Weathering time (days)	Test conditions	Compressive load (kN)	Compressive stress (MPa)	Shear load (kN)	Shear strength (MPa)	Internal friction angle	Cohesion (MPa)	Friction coefficient
0	Condition 1-1	10	5.72	14.84	8.48	42.22	3.28	0.91
	Condition 1-2	15	8.59	19.28	11.05			
	Condition 1-3	20	11.31	23.98	13.56			
	Condition 1-4	25	14.06	26.71	16.14			
7	Condition 2-1	10	5.73	11.84	6.78	42.92	1.60	0.99
	Condition 2-2	15	8.57	17.9	10.22			
	Condition 2-3	20	11.42	19.86	11.34			
	Condition 2-4	25	14.11	26.76	15.10			
14	Condition 3-1	10	5.72	9.96	5.70	40.02	1.07	0.84
	Condition 3-2	15	8.48	15.07	8.52			
	Condition 3-3	20	11.24	18.44	10.36			
	Condition 3-4	25	14.11	22.96	12.90			
21	Condition 4-1	10	5.72	8.87	4.99	40.02	0.67	0.78
	Condition 4-2	15	8.48	13.57	7.63			
	Condition 4-3	20	11.24	16.74	9.41			
	Condition 4-4	25	14.11	20.82	11.7			
28	Condition 5-1	10	5.72	7.98	4.49	40.02	0.38	0.74
	Condition 5-2	15	8.48	12.12	6.81			
	Condition 5-3	20	11.23	15.36	8.63			
	Condition 5-4	25	14.11	19.10	10.73			

Table 5: The mechanical parameters of rock specimen.

Rock type	Weathering time (days)	Tensile strength (MPa)	Compression strength (MPa)	Elastic modulus (GPa)	Poisson ratio	Internal friction angle	Cohesion (MPa)	Friction coefficient
Black shale	0	9.82	66.48	13.29	0.160	42.22	3.28	0.91
	7	6.91	39.51	7.96	0.295	42.92	1.60	0.99
	14	5.09	24.25	5.47	0.339	40.02	1.07	0.84
	21	4.02	15.29	4.02	0.379	40.02	0.67	0.78
	28	2.98	10.09	3.55	0.408	40.02	0.38	0.74

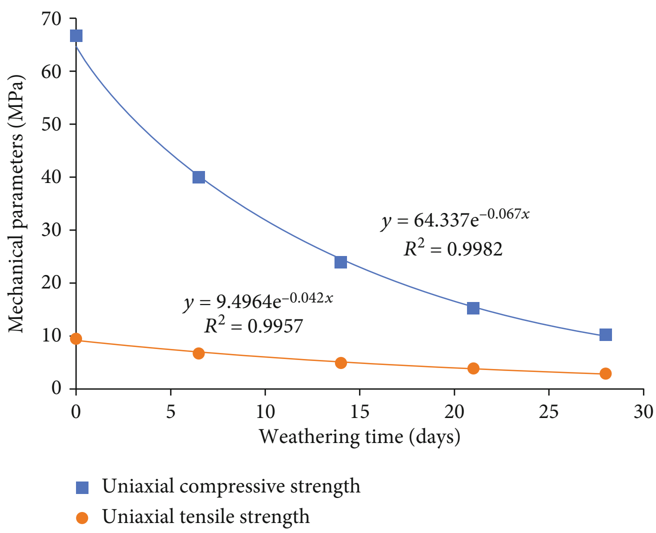

Figure 8: Average uniaxial tensile strength of the specimen under different weathering time.

The elastic modulus and Poisson's ratio values of the specimen at different weathering times are plotted in Figure 9. With the increasing of the weathering time, the elastic modulus values of the specimen gradually decreased, while the Poisson's ratio gradually increased. The change in the elastic modulus at the weathering time of zero and 28 days decreased by 2.74 times, while the Poisson's ratio value increased by 2.92 times. The trendlines of the variations of elastic modulus and Poisson's ratio values with the weathering time are plotted in Figure 8, characterized as the quadratic behavior. The determination coefficient (R^2) of the plotted trendlines are also provided.

The variations in the shear strength values at different weathering times while under different compressive stresses are displayed in Figure 10. It is clear that the correlations between shear strength values and the applied compressive at a particular weathering time were near a straight line. At a particular applied compressive stress, the shear strength of the specimens gradually decreased with the increasing of the weathering time. It is observed that the internal friction angle which is the inclination of the straight line remained consistent at different weathering times. The average internal friction angle at a different weathering time was around 42 degrees. The cohesion which is the intercept of the fitted straight line on the ordinate decreased with the increasing of the weathering time. As shown Figure 11, the cohesion of the specimens had a negative exponential relationship with the weather times. The cohesion of the specimen without the exposure to the environments (3.28 MPa) was around 9 times for the specimens at the weathering time of 28 days (0.38 MPa).

According to the comprehensive experimental tests and results analysis, the correlation function between the weathering time and the uniaxial tensile strength, uniaxial compression strength, modulus of elasticity, Poisson's ratio, and cohesion of rock specimens were obtained, as summarized in Table 6. The determination coefficient (R^2) of each of the correlation function is also provided. The uniaxial tensile strength, uniaxial compression strength, and cohesion of rock specimens were characterized as the negative exponential relationship with the weathering times. The modulus of elasticity has a negative quadratic relationship, while Poisson's ratio had a positive quadratic relationship with the weathering times.

4.2. Discussions. Momeni et al. [25] reported that the difference in the compressive strength and elastic modulus for the fresh and weathered rock is related to their petrographical properties. The existence of clay minerals in the rock was regarded as one of the most important parameters that affected the mechanical properties of the rock through weathering [12]. The black shale specimens used in this study is a typical type of sedimentary rock that formed by dehydration and cementation of clay. The experimental results in this study showed that the rock consisting of clay minerals could be easily softened by the weathering process evidenced by the small deformation modulus and poor antisliding stability. The decrease of compressive strength and elastic modulus of the sedimentary rock with the weathering time confirmed the previous findings and also suggested that the sedimentary rock was sensitive to the weathering grades. In fact, after only 7 days' weathering, the structure of the specimen was significantly damaged evidenced by the obvious decrease of the mechanical parameters.

The cumulative damage of the rock by the weathering time may result in the microcrack coalescence within the rock, which has a great influence on the time-dependent behavior of the rock. Typically, because of the sliding of the initial crack at the elastic deformation stage, microcrack initiated and propagated along the length of the initial crack [26–30]. From this aspect, it was hypothesized that the gradual development of the transverse and longitudinal microcracks coalescence in the specimens during the weathering process led to earlier microcrack initiation compared with the specimens without weathering. The existence of the microcrack coalescence produced during the weathering process could accelerate the crack propagation and result in the macroscopic failure of the rock at low-stress magnitudes. This observation could account for a positive relationship between the Poisson's ratio and weathering time. The development of microcrack coalescence during the weathering process accelerated the radial deformation during the loading process, which resulted in the positive quadratic relationship between the Poisson's ratio and weathering time.

During the failure processes, the direction of the crack initiation and propagation within the rock are randomly distributed. The initiation and propagation of microcracks can be predicted to some extent using the Griffith theory [31]. Other researchers reported that the friction coefficient which is used to describes the sliding friction at microcrack surfaces has important effects on the rock strength and proposed the modified Griffith criterion considering the friction coefficient [32]. The values of the friction coefficient were different along the surface of microcracks, and this value was determined by the extent of wear due to sliding [33–36]. From this aspect,

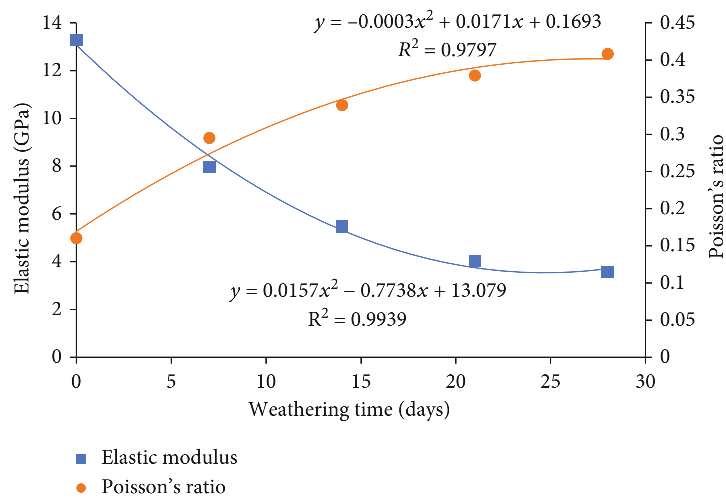

FIGURE 9: The relationship between the elastic modulus and Poisson's ratio with weathering time.

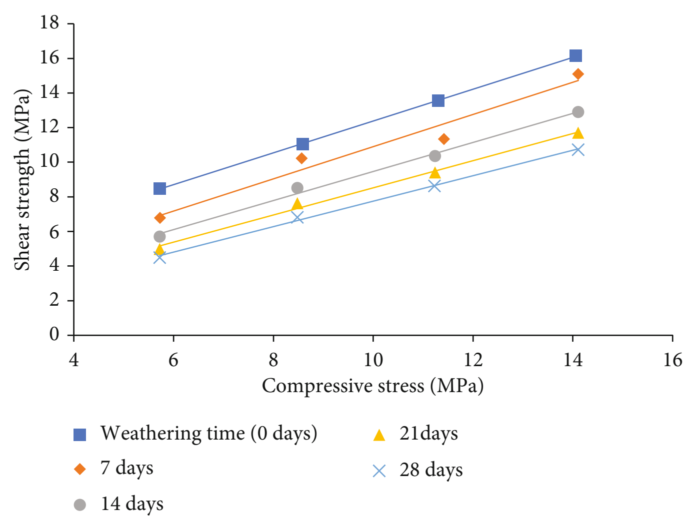

FIGURE 10: Variation in the shear strength under different compressive stress with weathering time.

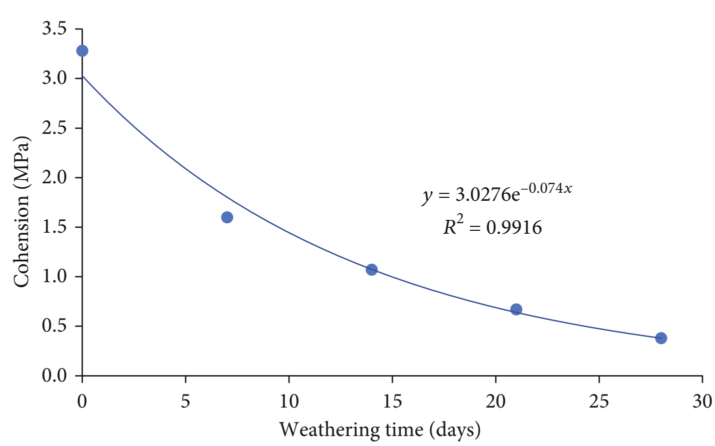

FIGURE 11: Variation in the cohesion of the specimen with weathering time.

Table 6: The correlation function between mechanical parameters and weathering time.

Rock type	Parameters	Type of functions	Fitting formula	Correlation coefficient (R^2)
Black shale	Uniaxial tensile strength	Exponential	$y = 9.4964e^{-0.042}x$	0.9957
	Uniaxial compression strength	Exponential	$y = 64.337e^{-0.067x}$	0.9982
	Elastic modulus	Quadratic	$y = 0.0157x^2 - 0.7738x + 13.079$	0.9939
	Poisson's ratio	Quadratic	$y = -0.0003x^2 + 0.0171x + 0.1693$	0.9797
	Cohesion	Exponential	$y = 3.0276e^{-0.074x}$	0.9916

the lower friction coefficient observed in the specimen with higher weathering grades could be attributed to cumulative damage and gradual development of the microcrack coalescence during the weathering process. The lower friction coefficient of the specimen with higher weathering grades led to the initiation and propagation of microcrack at lower stress conditions.

How to obtain accurate and reliable time-dependent behaviors of rock mass has always been an important topic for geotechnical engineering scholars. Conducting the durability tests for evaluating the long-term durability behavior of rock specimens is time-consuming as well as expensive. In this study, the time-dependent durability behaviors of the sedimentary rocks were assessed, and the ageing of the rock specimens that weathered in the natural state was examined. The degradation of the mechanical parameters of rock specimen with different weathering grades was evaluated through the comprehensive experimental programs. However, it should be noted that even though the rock specimen was taken from the site and weathered in the natural state, the selected rock specimens are with good integrity and do not contain or rarely contain the unique weak structural plane of the natural rock mass. The mechanical parameters tested in the laboratory cannot fully represent the mechanical characteristics of the natural rock mass. Therefore, its mechanical parameters need to be reduced in a certain proportion to be applied to the natural rock mass.

5. Conclusions

The paper presented the initial results from the extensive experimental programs to establish the time-dependent behaviors of the sedimentary rocks considering the effects of weathering. The Brazilian split tests, uniaxial compression tests, and direct shear tests have been carried out on the specimens that are exposed to the nature environments at different durations. It was identified that the uniaxial tensile strength, uniaxial compressive strength, and cohesion dramatically decreased with increasing weathering time, characterized as the negative exponential relationship in general. The elastic modulus had a negative quadratic relationship, while the Poisson's ratio had a positive quadratic relationship with the weathering times. It was suggested that the cumulative damage of the rock by the weathering time resulted in the microcrack coalescence within the rock. The existence of the microcrack coalescence facilitated the propagation of the microcracks and accelerated the radial deformation during the loading process. The friction coefficient decreased with the increasing of the weathering grades. The lower friction coefficient observed in the specimen with higher weathering grades led to the initiation and propagation of microcrack within the rock at lower stress conditions. The results and the proposed correlation between the long-term durability behavior of the sedimentary rocks and weathering grades improved the understanding of the roles of weathering on the mechanical properties which can be used in the design of the underground geotechnical engineering structures.

Data Availability

The data used to support the findings of this study are included within the article, and detailed data are available from the corresponding author upon request.

Conflicts of Interest

The authors declare that they have no conflicts of interest.

Acknowledgments

The work of this paper is financially supported by the National Natural Science Foundation of China (Grant number: 41702327, 41867033, 52004196), China Postdoctoral Science Foundation (Grant number: 2019M650144), State Key Laboratory of Safety and Health of Metal Mines (Grant number: zdsys2019-005), Shanxi Education Department (Grant number: 19JK0454), and Science and Technology Bureau of Beilin, Xi'an (GX2016).

References

[1] C. R. Windsor, "Rock reinforcement systems," *International Journal of Rock Mechanics and Mining Sciences*, vol. 34, no. 6, pp. 919–951, 1997.

[2] Z. T. Bieniawski, "Mechanism of brittle fracture of rock," *International Journal of Rock Mechanics and Mining Science and Geomechanics Abstracts*, vol. 4, no. 4, pp. 407–423, 1967.

[3] E. Hoek and Z. T. Bieniawski, "Brittle fracture propagation in rock under compression," *International Journal of Fracture Mechanics*, vol. 1, no. 3, pp. 137–155, 1965.

[4] M. H. Ghobadi and A. A. Momeni, "Assessment of granitic rocks degradability susceptive to acid solutions in urban area," *Environmental Earth Sciences*, vol. 64, no. 3, pp. 753–760, 2011.

[5] S. S. Wu, H. Chen, P. Craig et al., "An experimental framework for simulating stress corrosion cracking in cable bolts,"

Tunnelling and Underground Space Technology, vol. 76, pp. 121–132, 2018.

[6] P. Tapponnier and W. F. Brace, "Development of stress-induced microcracks in westerly granite," *International Journal of Rock Mechanics and Mining Science and Geomechanics Abstracts*, vol. 13, no. 4, pp. 103–112, 1976.

[7] S. S. Wu, J. Guo, G. Shi, J. Li, and C. Lu, "Laboratory-based investigation into stress corrosion cracking of cable bolts," *Materials*, vol. 12, no. 13, p. 2146, 2019.

[8] S. R. Wang, X. G. Wu, Y. H. Zhao, P. Hagan, and C. Cao, "Evolution characteristics of composite pressure-arch in thin bedrock of overlying strata during shallow coal mining," *International Journal of Applied Mechanics*, vol. 11, no. 3, article 1950030, 2019.

[9] Y. C. Li, C. Z. Wu, and B. A. Jang, "Effect of bedding plane on the permeability evolution of typical sedimentary rocks under triaxial compression," *Rock Mechanics and Rock Engineering*, vol. 53, pp. 5283–5291, 2020.

[10] Y. C. Li, C.'. Tang, D. Li, and C. Wu, "A new shear strength criterion of three-dimensional rock joints," *Rock Mechanics and Rock Engineering*, vol. 53, no. 3, pp. 1477–1483, 2020.

[11] S. S. Wu, H. L. Ramandi, H. Chen, A. Crosky, P. Hagan, and S. Saydam, "Mineralogically influenced stress corrosion cracking of rockbolts and cable bolts in underground mines," *International Journal of Rock Mechanics and Mining Sciences*, vol. 119, pp. 109–116, 2019.

[12] C. Gökceoğlu, R. Ulusay, and H. Sönmez, "Factors affecting the durability of selected weak and clay-bearing rocks from Turkey, with particular emphasis on the influence of the number of drying and wetting cycles," *Engineering Geology*, vol. 57, no. 3, pp. 215–237, 2000.

[13] A. Basu, T. B. Celestino, and A. A. Bortolucci, "Evaluation of rock mechanical behaviors under uniaxial compression with reference to assessed weathering grades," *Rock Mechanics and Rock Engineering*, vol. 42, no. 1, pp. 73–93, 2009.

[14] J. Q. Liu, W. Chen, T. Liu, J. Yu, J. Dong, and W. Nie, "Effects of initial porosity and water pressure on seepage-erosion properties of water inrush in completely weathered granite," *Geofluids*, vol. 2018, Article ID 4103645, 11 pages, 2018.

[15] S. S. Wu, J. Li, J. Guo, G. Shi, Q. Gu, and C. Lu, "Stress corrosion cracking fracture mechanism of cold-drawn high-carbon cable bolts," *Materials Science and Engineering*, vol. 769, article 138479, 2020.

[16] S. Wu, M. Northover, P. Craig, I. Canbulat, P. C. Hagan, and S. Saydam, "Environmental influence on mesh corrosion in underground coal mines," *International Journal of Mining, Reclamation and Environment*, vol. 32, no. 8, pp. 519–535, 2017.

[17] D. Arias, L. Pando, C. López-Fernández, L. M. Díaz-Díaz, and Á. Rubio-Ordóñez, "Deep weathering of granitic rocks: a case of tunnelling in NW Spain," *Catena*, vol. 137, pp. 572–580, 2016.

[18] M. Heidari, G. R. Khanlari, A. A. Momeni, and H. Jafargholizadeh, "The relationship between geomechanical properties and weathering indices of granitic rocks, Hamedan, Iran," *Geomechanics and Geoengineering*, vol. 6, no. 1, pp. 59–68, 2011.

[19] S. Ceryan, K. Zorlu, C. Gokceoglu, and A. Temel, "The use of cation packing index for characterizing the weathering degree of granitic rocks," *Engineering Geology*, vol. 98, no. 1-2, pp. 60–74, 2008.

[20] S. S. Wu, X. Zhang, J. Li, and W. Zhao, "Investigation for Influences of Seepage on Mechanical Properties of Rocks Using Acoustic Emission Technique," *Geofluids*, no. 6693920, 2020.

[21] M. Heidari, A. A. Momeni, and F. Naseri, "New weathering classifications for granitic rocks based on geomechanical parameters," *Engineering Geology*, vol. 166, pp. 65–73, 2013.

[22] A. A. Momeni, G. R. Khanlari, M. Heidari, A. A. Sepahi, and E. Bazvand, "New engineering geological weathering classifications for granitoid rocks," *Engineering Geology*, vol. 185, pp. 43–51, 2015.

[23] S. V. Alavi Nezhad Khalil Abad, A. Tugrul, C. Gokceoglu, and D. Jahed Armaghani, "Characteristics of weathering zones of granitic rocks in Malaysia for geotechnical engineering design," *Engineering Geology*, vol. 200, pp. 94–103, 2016.

[24] S. Qi, Z. Q. Yue, C. Liu, and Y. Zhou, "Significance of outward dipping strata in argillaceous limestones in the area of the Three Gorges reservoir, China," *Bulletin of Engineering Geology and the Environment*, vol. 68, no. 2, pp. 195–200, 2009.

[25] A. Momeni, S. S. Hashemi, G. R. Khanlari, and M. Heidari, "The effect of weathering on durability and deformability properties of granitoid rocks," *Bulletin of Engineering Geology and the Environment*, vol. 76, no. 3, pp. 1037–1049, 2017.

[26] L. N. Germanovich, R. L. Salganik, A. V. Dyskin, and K. K. Lee, "Mechanisms of brittle fracture of rock with pre-existing cracks in compression," *Pure and Applied Geophysics*, vol. 143, no. 1-3, pp. 117–149, 1994.

[27] S. S. Wu, H. Chen, H. Lamei Ramandi et al., "Investigation of cable bolts for stress corrosion cracking failure," *Construction and Building Materials*, vol. 187, pp. 1224–1231, 2018.

[28] N. Erarslan and D. J. Williams, "Mixed-mode fracturing of rocks under static and cyclic loading," *Rock Mechanics and Rock Engineering*, vol. 46, no. 5, pp. 1035–1052, 2013.

[29] S. R. Wang, X. G. Wu, J. H. Yang, J. Q. Zhao, and F. L. Kong, "Mechanical behavior of lightweight concrete structures subjected to 3D coupled static-dynamic loads," *Acta Mechanica*, vol. 231, no. 11, pp. 4497–4511, 2020.

[30] S. Mo, I. Canbulat, C. Zhang, J. Oh, B. Shen, and P. Hagan, "Numerical investigation into the effect of backfilling on coal pillar strength in highwall mining," *International Journal of Mining Science and Technology*, vol. 28, no. 2, pp. 281–286, 2018.

[31] A. M. Ferrero, "The shear strength of reinforced rock joints," *International Journal of Rock Mechanics and Mining Sciences*, vol. 32, no. 6, pp. 595–605, 1995.

[32] H. Sonmez, E. Tuncay, and C. Gokceoglu, "Models to predict the uniaxial compressive strength and the modulus of elasticity for Ankara Agglomerate," *International Journal of Rock Mechanics and Mining Sciences*, vol. 41, no. 5, pp. 717–729, 2004.

[33] S. Amini, H. N. Hosseinabadi, and S. A. Sajjady, "Experimental study on effect of micro textured surfaces generated by ultrasonic vibration assisted face turning on friction and wear performance," *Applied Surface Science*, vol. 390, pp. 633–648, 2016.

[34] J. Y. Cheng, H. W. Zhang, and Z. J. Wan, "Numerical simulation of shear behavior and permeability evolution of rock joints with variable roughness and infilling thickness," *Geofluids*, vol. 2018, Article ID 1869458, 11 pages, 2018.

[35] S. R. Wang, H. G. Xiao, Z. S. Zou, C. Cao, Y. H. Wang, and Z. L. Wang, “Mechanical performances of transverse rib bar during pull-out test,” *International Journal of Applied Mechanics*, vol. 11, no. 5, article 1950048, 2019.

[36] C. C. Wei, C. Zhang, I. Canbulat, A. Cao, and L. Dou, “Evaluation of current coal burst control techniques and development of a coal burst management framework,” *Tunnelling and Underground Space Technology*, vol. 81, pp. 129–143, 2018.